

Isotopic effects in two-body fragmentation process of water dications induced by electron-impact ionization

Xiaorui Xue(薛晓睿), Jiaqi Zhou(周家琪), Xintai Hao(郝鑫泰), Lei Wang(王磊), Peng Li(李鹏), Qibo Ma(马启博), and Xueguang Ren(任雪光)

Citation: Chin. Phys. B, 2025, 34 (**7**): 073401. DOI: 10.1088/1674-1056/add4fd
http://cpb.iphy.ac.cn; http://iopscience.iop.org/cpb

What follows is a list of articles you may be interested in

Fragmentation dynamics of nitric oxide induced by low-energy heavy ions

Zhixin Li(李志欣), Kaizhao Lin(林楷钊), Xiaolong Zhu(朱小龙), Zhiliang Li(李志亮), Hang Yuan(苑航), Yong Gao(高永), Dalong Guo(郭大龙), Dongmei Zhao(赵冬梅), Shaofeng Zhang(张少锋), and Xinwen Ma(马新文)
Chin. Phys. B, 2025, 34 (**5**): 053401. DOI: 10.1088/1674-1056/adbdc0

Momentum distributions of symmetric (H_2^+) and asymmetric (HeH^{2+}) molecular ions in a circularly polarized laser field under different ionization mechanisms

Xin-Yu Hao(郝欣宇), Shu-Juan Yan(闫淑娟), Ying Guo(郭颖), and Jing Guo(郭静)
Chin. Phys. B, 2024, 33 (**12**): 123401. DOI: 10.1088/1674-1056/ad7c2b

Vibronic effect study of $^1A_2$ state of H_2O and D_2O

Bei-Yuan Zhang(张倍源), Li-Han Wang(王礼涵), Jian-Hui Zhu(朱剑辉), Wei-Qing Xu(徐卫青), Zi-Ru Ma(马子茹), Xiao-Li Zhao(赵小利), Yong Wu(吴勇), and Lin-Fan Zhu(朱林繁)
Chin. Phys. B, 2024, 33 (**5**): 053401. DOI: 10.1088/1674-1056/ad24d9

Formation of nanobubbles generated by hydrate decomposition: A molecular dynamics study

Zilin Wang(王梓霖), Liang Yang(杨亮), Changsheng Liu(刘长生), and Shiwei Lin(林仕伟)
Chin. Phys. B, 2023, 32 (**2**): 023101. DOI: 10.1088/1674-1056/ac786a

Development of an electronic stopping power model based on deep learning and its application in ion range prediction

Xun Guo(郭寻), Hao Wang(王浩), Changkai Li(李长楷),Shijun Zhao(赵仕俊), Ke Jin(靳柯), and Jianming Xue(薛建明)
Chin. Phys. B, 2022, 31 (**7**): 073402. DOI: 10.1088/1674-1056/ac4e0c

---

SPECIAL TOPIC — Ultrafast physics in atomic, molecular and optical systems

Isotopic effects in two-body fragmentation process of water dications induced by electron-impact ionization

Xiaorui Xue(薛晓睿), Jiaqi Zhou(周家琪)†, Xintai Hao(郝鑫泰), Lei Wang(王磊), Peng Li(李鹏), Qibo Ma(马启博), and Xueguang Ren(任雪光)‡

Ministry of Education Key Laboratory for Nonequilibrium Synthesis and Modulation of Condensed Matter, School of Physics, Xi'an Jiaotong University, Xi'an 710049, *China*

(Received 28 February 2025; revised manuscript received 19 April 2025; accepted manuscript online 7 May 2025)

The two-body fragmentation dynamics of water isotopologues dications (H_2O^{2+}, HOD^{2+}, and D_2O^{2+}) induced by 200 eV electron impact is investigated. Two fragment ions and an emitted electron are detected in coincidence, and their momentum vectors are determined by employing a reaction microscope. The complete kinematical information of four two-body fragmentation channels of $H^+ + OH^+$, $H^+ + OD^+$, $D^+ + OH^+$, and $D^+ + OD^+$ is obtained. By analyzing the projectile energy-loss spectrum, the initial electronic state of the two-body dissociation channel is determined. Upon examining the kinetic energy release (KER) distributions of the four fragmentation channels, a clear difference is found between the two-body fragmentation channel $H^+ + OD^+$ and the other three channels. The isotopic effect in the two-body fragmentation is demonstrated by the analysis of the relative yields of the two-body fragmentation channels originating from different isotopologues, which shows preferential cleavage of the O–H bond over the O–D bond. These results provide deeper insight into the microscopic dynamic mechanisms in water radiolysis.

Keywords: isotopic effect, two-body fragmentation dynamics, kinetic energy release

PACS: 34.50.Bw, 31.15.xv, 32.10.Bi, 07.77.Gx

DOI: 10.1088/1674-1056/add4fd **CSTR:** 32038.14.CPB.add4fd

1. Introduction

The isotopic effect is a key concept in chemistry and physics and is related to critical reactions in biochemistry and physics, such as photosynthesis and nuclear fusion.[1–10] Serving as the solvent for biochemical reactions, the ionization and dissociation of water molecules form highly reactive radicals,[11] which can further drive cascading radiative reactions. These processes are critical in diverse fields, including radiation damage,[12] radiation diagnosis and therapy,[13] and corrosion in nuclear reactors.[14] The three isotopomers of water, which are normal water (H_2O), semi-deuterated water (HOD), and fully deuterated water (D_2O), provide a three-atom prototype for studying the isotopic effect. Minute differences in nuclear mass among isotopomers can cause noticeable changes in radiolysis rates, the energy, and yields of radicals.[15,16]

The double ionization of water is a fundamental process in water radiolysis.[17–21] Water dications are typically unstable and tend to dissociate into smaller pieces due to Coulomb repulsion between charges. One of the dominant processes observed in all dissociation events is the O–H bond cleavage, leading to the formation of a proton and a hydroxyl cation. This process arises from two distinct relaxation mechanisms: direct double ionization-induced dissociation and a sequential mechanism where single ionization of the water molecule is followed by rapid dissociation into a proton and an autoionizing hydroxyl radical (OH^*).[22,23] In the study of direct double ionization dissociation, the HOD^{2+} dications exhibit preferential cleavage of the O–H bond over the O–D bond[24,25] and the kinetic energy release (KER) dissociating into $H^+ + OD^+$ is higher than that of $D^+ + OH^+$.[26] Theoretical calculations indicate that the ratio between the populations of two channels and the KER difference are primarily governed by saddle points at equal values of the R_{OH} distance in the potential energy surfaces (PESs) of molecular states.[27–29] Based on the calculated PESs, the ratio and KER of the two channels are also predicted. In experiments, the isotopic ratios are determined by detecting the counts of $H^+ + OD^+/D^+ + OH^+$ ion pairs in coincidence.[25,26] However, there are significant disparities not only between theoretical predictions and experimental results but also among different experimental outcomes, which require refined measurements to address these issues.

In the present work, we study the two-body fragmentation dynamics of three water isotopologues. In the experiment, two electrons are removed from the water molecules by 200 eV electron impact. The electron-impact experiments are motivated by the abundant generation of secondary electrons dur-

†Corresponding author. E-mail: zhoujiaqi@xjtu.edu.cn

‡Corresponding author. E-mail: renxueguang@xjtu.edu.cn

© 2025 Chinese Physical Society and IOP Publishing Ltd. All rights, including for text and data mining, AI training, and similar technologies, are reserved.

ing water radiolysis, highlighting the critical role of electron-driven processes in radiation-induced damage.[14] Two fragment ions and one electron are measured in triple coincidence, and the momentum vector of each particle is determined. Particular attention is paid to four two-body dissociation channels with the emission of proton/deuterated proton from the dications (H_2O^{2+}, HOD^{2+}, and D_2O^{2+}). The projectile energy-loss (E_{loss}) spectrum and KER spectrum are obtained, which enable us to reveal the initial state and fragmentation details of the two-body channels. By comparing the KER distributions and the relative ratios of different dissociation channels originating from three water isotopologues, we reveal the isotopic differences in the two-body dissociation process of doubly ionized water molecules.

2. Experiment

The experiment was performed using an advanced reaction microscope that allows the coincidence measurement of fragment ions and electrons.[30–32] A brief overview of the setup is provided here, as detailed descriptions are available elsewhere.[32,33] In the reaction region, a pulsed electron beam with an energy of 200 eV intersects with a supersonic gas jet, leading to the ionization of the target. The pulsed electron beam, with a duration of $\Delta T \approx 0.5$ ns and an energy width of $\Delta E_0 \approx 0.5$ eV, is generated by a pulsed ultraviolet laser beam ($\lambda = 266$ nm) irradiating a tantalum photocathode. The supersonic gas jet, consisting of a 50:50 mixture of H_2O and D_2O, leading to approximately 25% H_2O, 25% D_2O, 50% HOD, is carried by helium into the reaction chamber through a 30-μm nozzle and a two-stage differential pumping system. A homogeneous electric field (1.5 V/cm) and magnetic field (6.8 Gauss) guide the electrons onto microchannel plate (MCP) detectors with delay-line position readout. The scattered electrons at small scattering angles in the near forward direction can be detected completely. Since the fragment ions typically carry higher momenta, 4π collection of ions requires a higher electric field (25 V/cm). This is obtained through a pulsed-field generator after the electron extraction. The unscattered electron beam is directed through a hole in the electron detector without generating a signal. During offline analysis, the three-dimensional momentum vector of each detected particle is reconstructed from the measured time of flight (TOF) and position.

3. Results and discussion

In the experiment, the generated ion fragments and electrons from three isotopologues of water (H_2O, HOD, and D_2O) are measured in coincidence, and the mass-to-charge ratios and three-dimensional momentum vectors of fragment ions are determined. The dissociation channels originating from three water isotopologues are identified by the TOF correlation map between two detected fragment ions, as shown in Fig. 1. These channels display a sharp diagonal structure with a slope of -1, due to the back-to-back emission of two cations with equal momentum magnitude but opposite directions. Besides, the shadow structures are observed in the upper-right quadrant of each channel, which originate from the sequential process where single ionization of the water molecule is followed by rapid dissociation into a proton and an autoionizing hydroxyl radical (OH^*).[22,23,34] Here, we focus on four complete two-body Coulomb explosion channels:

$$HOD^{2+} \rightarrow H^+ + OD^+, \quad (1)$$

$$HOD^{2+} \rightarrow D^+ + OH^+, \quad (2)$$

$$H_2O^{2+} \rightarrow H^+ + OH^+, \quad (3)$$

$$D_2O^{2+} \rightarrow D^+ + OD^+. \quad (4)$$

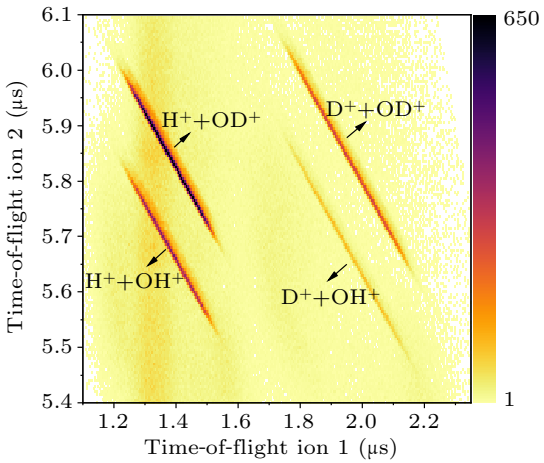


Fig. 1. Experimental time-of-flight correlation spectrum of two measured cations. Four two-body dissociation channels of water dications (H_2O^{2+}, HOD^{2+}, and D_2O^{2+}) are identified.

In our measurement, the scattered electrons are detected in coincidence with the $H^+ + OH^+$ ion pair. The E_{loss} spectrum associated with the two-body dissociation channel is obtained, which allows us to determine the initial state of the dissociation channel. The projectile energy loss is defined as the incident projectile energy E_0 minus the scattered electron energy E_1 ($E_{loss} = E_0 - E_1$). The energy loss spectrum is calibrated using the single ionization of helium with $E_{loss}[He^+] = 24.6$ eV. The energy-loss spectrum of the $H^+ + OH^+$ channel is displayed in Fig. 2. The minimum energy leading to specific ionization channels can be determined from the onsets of the E_{loss} spectrum. The onset value is determined as approximately 34.5 eV (refer to the arrow in Fig. 2), which lies below the vertical double-ionization threshold of H_2O (39 eV).[24] This is consistent with the threshold (34.4 eV) of the indirect dissociative double-ionization channel reported in photoionization experiments.[22,35–37] In this process, neutral water molecules are first singly ionized and simultaneously excited, which is followed by the dissociation into a proton and

an excited OH^* fragment. The OH^* fragment subsequently autoionizes to reach the $X^3\Sigma^-$ ground state leading to OH^+ once the proton is far enough away that the autoionization channel becomes energetically accessible.[22]

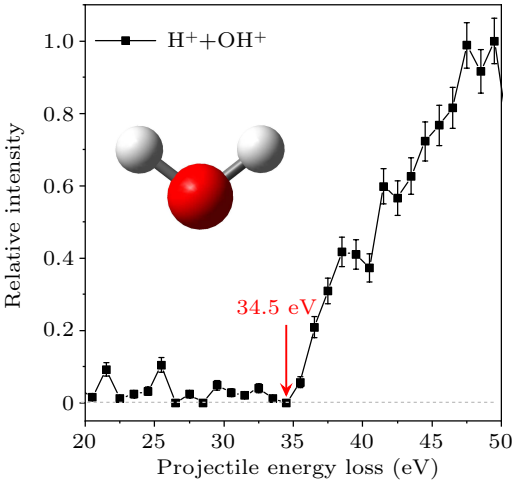


Fig. 2. Projectile energy-loss spectrum for two-body dissociation channel $H^+ + OH^+$. The arrow represents the onset of the channel.

To unravel the fragmentation dynamics of water dication (H_2O^{2+}, HOD^{2+}, and D_2O^{2+}), the KER spectra are measured for four two-body fragmentation channels. The KERs are normalized to emphasize the variation of the peak position and width of the KER distribution. The KER distributions are consistent with previous experimental measurements.[34,38] As shown in Fig. 3, the KER distributions of channels (2)–(4) are almost identical, with a peak value at about 6.3 eV and a shoulder at around 4.0 eV. It has been demonstrated that the low KER component is produced via an indirect two-step process, that is, an autoionization that takes place outside of the vertical Franck–Condon region. The high KER component is regarded as the contribution from higher dication states.[22,24,37,39,40] However, for channel (1), only the shoulder is identical to other channels, while the main peak shifts to a larger value ($\sim$ 6.7 eV) and exhibits a wider distribution. This indicates that the isotopic effect has a minimal impact on the sequential dissociation process, being primarily observed in the direct dissociation channels.

The KER difference between them can be explained both by the initial phase-space distribution correlations and the vibrational energy of the final residual fragment. In the $H^+ + OD^+$ and $D^+ + OD^+$ channels, the vibrational energy of the final OD^+ ion is identical. The differences in KER arise from the initial phase-space distribution of neutral molecules, which is related to their vibrational frequency and reduced mass.[26] These parameters for HOD and D_2O molecules are different.[41,42] For the two channels of HOD^{2+} ions, the initial energy of the parent dication leading to the $H^+ + OD^+$ is higher than the $D^+ + OH^+$ channel.[26] Furthermore, for the same vibrational energy levels of OH^+ and OD^+, the vibrational energy of OH^+ is higher than that of OD^+ by approximately 0.45 eV.[26] These lead to a higher KER of the $H^+ + OD^+$ channel. For the broad distribution of the $H^+ + OD^+$ channel, it originates from the different PESs configurations of different states. According to the calculated energy levels and fragmentation schemes of doubly charged water molecules with *ab initio* multi-reference configuration interaction method,[27] the lowest triplet state (X^3A'') and the three lowest singlet states ($1^1A'$, $1^1A''$, $2^1A'$) can lead to the $H^+ + OD^+$ and $D^+ + OH^+$ channels. The X^3A'' and $1^1A''$ states mainly contribute to the $H^+ + OD^+$ channel. The relatively steep slope of the PES of these two states leads to the broader KER distributions. While the $D^+ + OH^+$ channel mainly originates from the $1^1A'$ state, whose PES presents a shallow minimum around $R_{OH} = 2.3$ a.u., meaning the surface is quite flat in the Franck-Condon area. The repulsive force between H^+/D^+ and OD^+/OH^+ is smaller than that between X^3A'' and $1^1A''$ states, which leads to the narrower KER distribution.

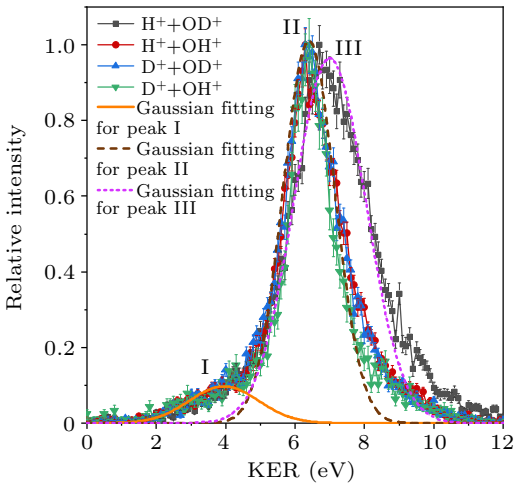


Fig. 3. The measured kinetic energy release spectrum for channels (1)–(4) with multipeak Gaussian fitting results. These curves are normalized to unity at the maximum.

Additionally, it is noteworthy that, unlike H_2O^{2+}, HOD^{2+} exhibits a preferred O–H bond dissociation. This can be readily understood as the O–H bond has a higher vibrational frequency than the O–D bond. Nevertheless, to quantitatively determine this tendency, it is necessary to precisely determine the ratio of the $H^+ + OD^+$ channel to the $D^+ + OH^+$ channel. In our experiments, the supersonic cold target contains H_2O, HOD, and D_2O. Therefore, we can simultaneously determine the yields of four two-body channels. The channel yields are determined by counting the channel events in coincidence measurement and normalized with the branching ratio of parent molecules in the gas target. The branching ratio is determined to be about $49.48\% \pm 0.11\% : 26.17\% \pm 0.09\% : 24.34\% \pm 0.08\%$ by the yield of the cations (HOD^+, H_2O^+ and D_2O^+). During counting statistics, we have taken into account the correction for detection efficiency for different ions,

which mainly depends on the incident energy, charge state, and mass for the individual ionic species.[43] The kinetic energies of the ions are increased at the time of impact on the MCP to increase the detection effciency, which are about 2200 eV for cation. Accordingly, the detection efficiencies for the water cations H_2O^+, HOD^+, and D_2O^+ are 0.474, 0.470, and 0.466, respectively. At the same time, for the lightest proton/deuterated proton, the detection efficiency has been determined to be 0.582, while the detection efficiency of the hydroxyl cations is 0.479 for OH^+, and 0.474 for OD^+.[43]

The relative yield of two-body fragmentation channels of water dications is displayed in Fig. 4. The yield of $D^+ + OH^+$ channel is used as a reference standard, the yields of the other three channels have been normalized to the $D^+ + OH^+$ channel. The results indicate that the relative yield of the $D^+ + OD^+$ is the highest, while the yield of the $D^+ + OH^+$ channel is the lowest. For HOD^{2+} dications, the yield of the $H^+ + OD^+$ channel is significantly higher than that of the $D^+ + OH^+$ channel, which shows that the cleavage of the O–H bond is more likely than that of the O–D bond by a factor of about 5.7 for the HOD^{2+}. The dominance of the $H^+ + OD^+$ channel can be understood by the following simple picture. The mass of D^+ is heavier than H^+, so the vibrational effect has larger influence on H^+ than on D^+.[44] The lighter H^+ fragment is accelerated more than the D^+ ion. The O–H distance thus increases faster than the O–D distance, making the trapping of OD^+ more likely than the reverse process. As a consequence, the competition between O–H and O–D bond elongation results in the H^+ reaching a larger distance from the O atom, while the D^+ ion stays, on average, in closer vicinity of the O atom and is trapped in the well of the OD^+ potential. Therefore, H^+ can be lost more easily, leading preferentially to the formation of the OD^+ ion.

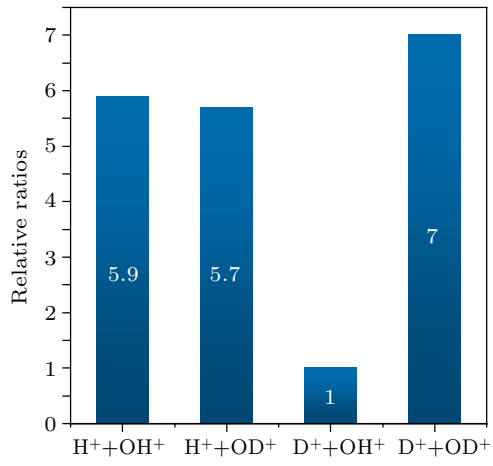


Fig. 4. The yield ratios of four two-body dissociation channels. The yield of $D^+ + OH^+$ is used as the reference standard for double ionization of water molecules (H_2O, HOD, and D_2O), with the value being set to 1.

From a theoretical point of view, accurate calculations have been published on the PESs of the ground and excited states of water dication.[27,45–47] The calculations presented the dependence of the isotopic ratio between two channels on the multiplicity of the HOD^{2+} molecular state. For example, the isotopic ratio for the ground triplet state was calculated to be 8.6, whereas for the first and second singlet states the ratios were found to be 3 and 15.7, respectively.[27] The discrepancy in the ratios between theoretical calculations and experimental results also indicates that the isotopic ratio in our experiments is an average value due to the population of the ground and several excited states. The initial rotational and vibrational states of the HOD molecule have also been proven to play an important role in the dissociation dynamics of the doubly ionized molecules.[28,48] With a prior vibrational excitation of the O–H or O–D mode, the branching ratio will increase or decrease correspondingly, which provides a possibility to selectively dissociate a water molecule into respective channels by simply exciting its vibrational modes.[28]

Taking a comprehensive view, both $H^+ + OD^+$ channel and $D^+ + OH^+$ channel contribute to the two-body dissociation of HOD^{2+}, which can be determined as the sum of the relative yields of the two channels, amounting to 6.7. The total relative yields are compared with the two-body dissociation yields of H_2O^{2+} (5.9) and D_2O^{2+} (7), it is suggested that the presence of deuterium atoms in water molecules also enhances the yield of the two-body dissociation channels. The differences in total relative yields also reflect the isotopic effect in the dissociation of water molecules.

4. Conclusion

To summarize, we have studied the two-body fragmentation dynamics of water dications (H_2O^{2+}, HOD^{2+}, and D_2O^{2+}) induced by 200 eV electron-impact. The complete two-body dissociation channels $H^+ + OH^+$, $H^+ + OD^+$, $D^+ + OH^+$, and $D^+ + OD^+$ are identified by the multiparticle coincidence measurements. Two ionic fragments and an emitted electron are measured in coincidence and their momentum vectors as well as kinetic energies are obtained. According to the projectile energy loss spectrum, the initial electronic state corresponding to the two-body dissociation channel is determined. Two fragmentation mechanisms of water dications are identified, including the direct double ionization dissociation and the sequential process. For the latter, single ionization of water molecule is followed by dissociation into a proton and an autoionizing OH^*. By comparing the measured KER of four two-body channels, it is found that the $H^+ + OD^+$ channel has a higher and broader KER distribution. Focusing on the two-body fragmentation of the water isotopologues, the dissociation of HOD molecules exhibits a strong isotopic preference for the cleavage of the O–H bond over the O–D bond. We find an isotopic branching ratio defined as the yield of $H^+ + OD^+$ over $D^+ + OH^+$ dissociations of 5.7. At the same time, the

relative yields of $H^+ + OH^+$ and $D^+ + OD^+$ are determined as 5.9 and 7, respectively. Our study provides a powerful way to investigate the isotopic effect of water molecules. By analyzing the isotopic difference in the two-body fragmentation of isotopologues of water induced by electron impact, we gain a deeper understanding of the dynamic mechanisms in water radiolysis.

Acknowledgements

Project supported by the National Natural Science Foundation of China (Grant Nos. 12325406, 92261201, 12404305, and 11974272), the Shannxi Province Natural Science Fundamental Research Project (Grant Nos. 2023JC-XJ-03 and 23JSQ013), and the Fundamental Research Funds for the Central Universities (Grant No. xzy022024040).

References

[1] Haberlandt R 2010 *Isot. Environ. Health. Stud.* **46** 400
[2] Goldstein M J 1966 *Science* **154** 1616
[3] Buchachenko A L 2013 *J. Phys. Chem. B* **117** 2231
[4] Bigeleisen J 1965 *Science* **147** 463
[5] Chao Y, Liang C, Yang Y, Wang G L, Maiti D, Tian L, Wang F, Pan W, Wu S, Yang K and Liu Z 2018 *ACS Nano* **12** 7519
[6] Eliezer S, Henis Z, Martínez-Val J M and Vorobeichik I 2000 *Nucl. Fusion* **40** 195
[7] Kahsai A W, Rajagopal S, Sun J P and Xiao K H 2014 *Nat. Protoc.* **9** 1301
[8] Wu D, Wei J, Dong T J, Zu C Y, Xia Y and Yin J P 2025 *Chin. Phys. B* **34** 023101
[9] Shi M H, Huang H, Lu C X, Pan S Z, Zhou L R, Jiang Z J, Ni H C, Zhang W B and Wu J 2024 *Phys. Rev. X* **14** 041001
[10] Zhao J, Xu T, Zhang L L and Wang L F 2020 *Chin. Phys. B* **29** 023105
[11] Olivera G H, Caraby C, Jardin P, Cassimi A, Adoui L and Gervais B 1998 *Phys. Med. Biol.* **43** 2347
[12] Boudaïffa B, Cloutier P, Hunting D, Huels M A and Sanche L 2000 *Science* **287** 1658
[13] Baumann M, Krause M, Overgaard J, Debus J, Bentzen S M, Daartz J, Richter C, Zips and Bortfeld T 2016 *Nat. Rev. Cancer* **16** 234
[14] Garrett B C, Dixon D A, Camaioni D M, *et al.* 2005 *Chem. Rev.* **105** 355
[15] Tarek M and Tobias D J 2002 *Phys. Rev. Lett.* **88** 138101
[16] Chen M H, Zheng L X, Santra B, Ko H Y, DiStasio R A J, Klein M L, Car R and Wu X F 2018 *Nat. Chem.* **10** 413
[17] Loh Z H, Doumy G, Arnold C, *et al.* 2020 *Science* **367** 179
[18] Svoboda V, Michiels R, Aaron C, *et al.* 2020 *Science Advances* **6** eaaz0385
[19] Lin M F, Singh N, Liang S, Mo M, Nunes J P F, Ledbetter K, Yang J, Kozina M, Weathersby S, Shen X, Cordones A A, Wolf T J A, Pemmaraju C D, Ihme M and Wang X J 2021 *Science* **374** 92
[20] Ren X G, Wang E L, Zhou J Q, Jia, S K, Wang X, Xue X R and Dorn A 2023 *Phys. Rev. A* **108** 052814
[21] Ren X G, Hossen K, Jia S K, Zhou J Q, Xue X, Pfeifer T and Dorn A 2024 *Phys. Rev. A* **110** 042801
[22] Sann H, Jahnke T, Havermeier T, Kreidi K, Stuck C, Meckel M, Schöffler M S, Neumann N, Wallauer R, Voss S, Czasch A, Jagutzki O, Weber Th, Schmidt-Böcking H, Miyabe S, Haxton D J, Orel A E, Rescigno T N and Dörner R 2011 *Phys. Rev. Lett.* **106** 133001
[23] Reedy D, Williams J B, Gaire B, Gatton A, Weller M, Menssen A, Bauer T, Henrichs K, Burzynski P, Berry B, Streeter Z L, Sartor J, Ben-Itzhak I, Jahnke T, Dörner R, Weber T and Landers A L 2018 *Phys. Rev. A* **98** 053430
[24] Richardson P J, Eland J H D, Fournier P G and Cooper D L 1986 *J. Chem. Phys.* **84** 3189
[25] Sayler A M, Leonard M, Carnes K D, Cabrera-Trujillo R, Esry B D and Ben-Itzhak I 2006 *J. Phys. B: At. Mol. Opt. Phys.* **39** 1701
[26] Legendre S, Giglio E, Tarisien M, Cassimi A, Gervais B and Adoui L 2005 *J. Phys. B: At. Mol. Opt. Phys.* **38** L233
[27] Gervais B, Giglio E, Adoui L, Cassimi A, Duflot D and Galassi M E 2009 *J. Chem. Phys.* **131** 024302
[28] Dey D and Tiwari A K 2016 *J. Phys. Chem. A* **120** 2629
[29] Akagi H, Fukazawa H, Yokoyama K and Yokoyama A 2005 *J. Chem. Phys.* **123** 184305
[30] Ullrich J, Moshammer R, Dorn A, Dörner R, Schmidt L Ph H and Schmidt-Böcking H 2003 *Rep. Prog. Phys.* **66** 1463
[31] Dörner R, Mergel V, Jagutzki O, Spielberger L, Ullrich J, Moshammer R and Schmidt-Böcking H 2000 *Phys. Rep.* **330** 95
[32] Zhou J Q, Jia S K, Hu X Q, Wang E L, Xue X R, Wu Y, Wang J G, Dorn A and Ren X G 2023 *Phys. Rev. A* **130** 233001
[33] Zhou J Q, Yu X T, Luo S Z, Xue X R, Jia S K, Zhang X Y, Zhao Y T, Hao X T, He L H, Wang C C, Ding D J and Ren X G 2022 *Nat. Commun.* **13** 5335
[34] Muranaka T 2007 *Fragmentation Dynamics of Triatomic Molecules: Contribution of Geometry* (Ph.D. Dissertation) (Caen: Université de Caen)
[35] Eland J H D 2006 *Chem. Phys.* **323** 391
[36] Carlson T A, Gerard P, Krause M O, Grant V W, Taylor J W and Grimm F A 1986 *J. Chem. Phys.* **84** 4755
[37] Winkoun D, Dujardin G, Hellner L and M J Besnard 1988 *J. Phys. B: At. Mol. Opt. Phys.* **21** 1385
[38] McCracken G A and Bucksbaum P H 2020 *J. Chem. Phys.* **152** 134308
[39] King S J and Price S D 2008 *Int. J. Mass Spectrom.* **277** 84
[40] Alvarado F, Hoekstra R and Schlathölter T 2005 *J. Phys. B: At. Mol. Opt. Phys.* **38** 4085
[41] Benedict W S, Gailar N, and Plyler E K 1956 *J. Chem. Phys.* **24** 1139
[42] Shi S P, Zhang Q, Zhang L, Wang R, Zhu Z H, Jiang G and Fu Y B 2011 *Chin. Phys. B* **20** 063102
[43] Krems M, Zirbel J, Thomason M and DuBois R D 2005 *Rev. Sci. Instrum.* **76** 093305
[44] Zhang B Y, Wang L H, Zhu J H, Xu W Q, Ma Z R, Zhao X L, Wu Y and Zhu L F 2015 *Chin. Phys. B* **33** 053401
[45] Van Huis T J, Wesolowski S S, Yamaguchi Y and Schaefer III H F 1999 *J. Chem. Phys.* **110** 11856
[46] Bunker P R, Bludský O, Jensen P, Wesolowski S S, Van Huis T J, Yamaguchi Y and Schaefer H F 1999 *J. Mol. Spectrosc.* **198** 371
[47] Nobusada K and Tanaka K 2000 *J. Chem. Phys.* **112** 7437
[48] Martin S, Chen L, Brédy R, Bernard J and Cassimi A 2015 *J. Chem. Phys.* **142** 094306